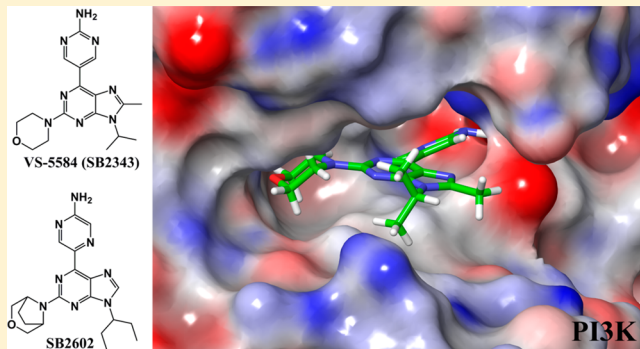


Structure and Ligand-Based Design of mTOR and PI3-Kinase Inhibitors Leading to the Clinical Candidates VS-5584 (SB2343) and SB2602

Anders Poulsen,* Harish Nagaraj, Angeline Lee, Stéphanie Blanchard, Chang Kai Soh, Dizhong Chen, Haishan Wang, Stefan Hart, Kee Chuan Goh, Brian Dymock, and Meredith Williams

S*BIO Pte Ltd, 1 Science Park Road, #05-09 The Capricorn, Singapore Science Park II, Singapore, Singapore 117 528

ABSTRACT: Phosphoinositide 3-kinases (PI3Ks) and the mammalian target of rapamycin (mTOR) act as critical effectors in a commonly deregulated cell signaling pathway in human cancers. The abnormal activation of the PI3K/mTOR pathway has been shown to play a role in initiation, progression, and metastasis of human tumors. Being one of the most frequently activated pathways in cancer, much effort has been directed toward inhibition of the PI3K/mTOR pathway as a novel oncology therapy. Previous work by a number of groups has revealed several selective PI3K and dual mTOR/PI3K inhibitors. However, there are few reports of therapeutic agents with a pan-PI3K/mTOR inhibitory profile within a narrow concentration range. We therefore initiated a drug discovery project with the aim of discovering dual mTOR/PI3K inhibitors which would equipotently inhibit the 4 isoforms of PI3K, α , β , γ , and δ , and mTOR a compelling profile for powerful blockage of the PI3K/mTOR pathway. A pharmacophore model was generated and used for designing a series of novel compounds, based on a purine scaffold, which potently inhibited mTOR and PI3Ks. These compounds contained a phenol headgroup essential for binding to the target proteins. Early efforts concentrated on finding replacements for the phenol as it was rapidly conjugated resulting in a short half-life *in vivo*. Compounds with a variety of headgroups were docked into the PI3K α and mTOR ATP-binding sites, and aminopyrimidine and aminopyrazine were found to make excellent phenol replacements. Further structure guided optimization of side chains in the 8- and 9-positions of the purine resulted in potent inhibitors with good PKDM properties. As the PI3 kinases play a role in insulin signaling, it is believed that targeting mTOR selectively may give the benefit of blocking the AKT-pathway while avoiding the potential side effects associated with PI3K inhibition. As a result we designed a further series of selective mTOR kinase inhibitors. The project was successfully concluded by progressing both a dual mTOR/PI3K inhibitor, SB2343, and a selective mTOR inhibitor, SB2602, into preclinical development. SB2343 has since entered phase 1 clinical development as VS-5584.



1. INTRODUCTION

The phosphatidylinositol 3-kinase (PI3K) family constitutes a group of lipid kinases that convert phosphatidylinositol-4,5-bisphosphate to phosphatidylinositol-3,4,5-trisphosphate. This conversion initiates a signaling pathway crucial to many aspects of cell growth and survival, including divergent physiological processes such as cell cycle progression, differentiation, transcription, translation, and apoptosis.¹ Furthermore, PI3K is a crucial regulator of angiogenesis and enhanced metabolic activity in tumors.² PI3K also modulates the activity of mammalian target of rapamycin (mTOR) by negative regulation of the tuberous sclerosis 1/2 (TSC1/2) complex.³ The PI3K/mTOR pathway is the most commonly activated signaling pathway in human cancer.⁴ Dysregulation, either through multiple upstream receptor classes, amplification of PI3K, deletion of phosphatase and tensin homologue (PTEN) or activating mutations has been closely linked to the development and progression of a wide range of cancers. Furthermore, acquired resistance to targeted therapies such as

receptor tyrosine kinase inhibitors (RTKi) or mitogen-activated protein kinase kinase inhibitors (MEKi) has been seen in recent clinical trials, and these have been attributed to increased PI3K/mTOR signaling.^{2,5} These findings have generated intense interest in the development of small-molecule modulators of key proteins in this cascade, including the various PI3K isoforms and mTOR. The structural homology of the adenosine triphosphate (ATP) binding sites within the PIKK (phosphatidylinositol 3-kinase-related kinases) family has enabled the discovery of small molecule inhibitors with varying degrees of activity against mTOR and the isoforms of the class I PI3Ks.

Received: August 10, 2014



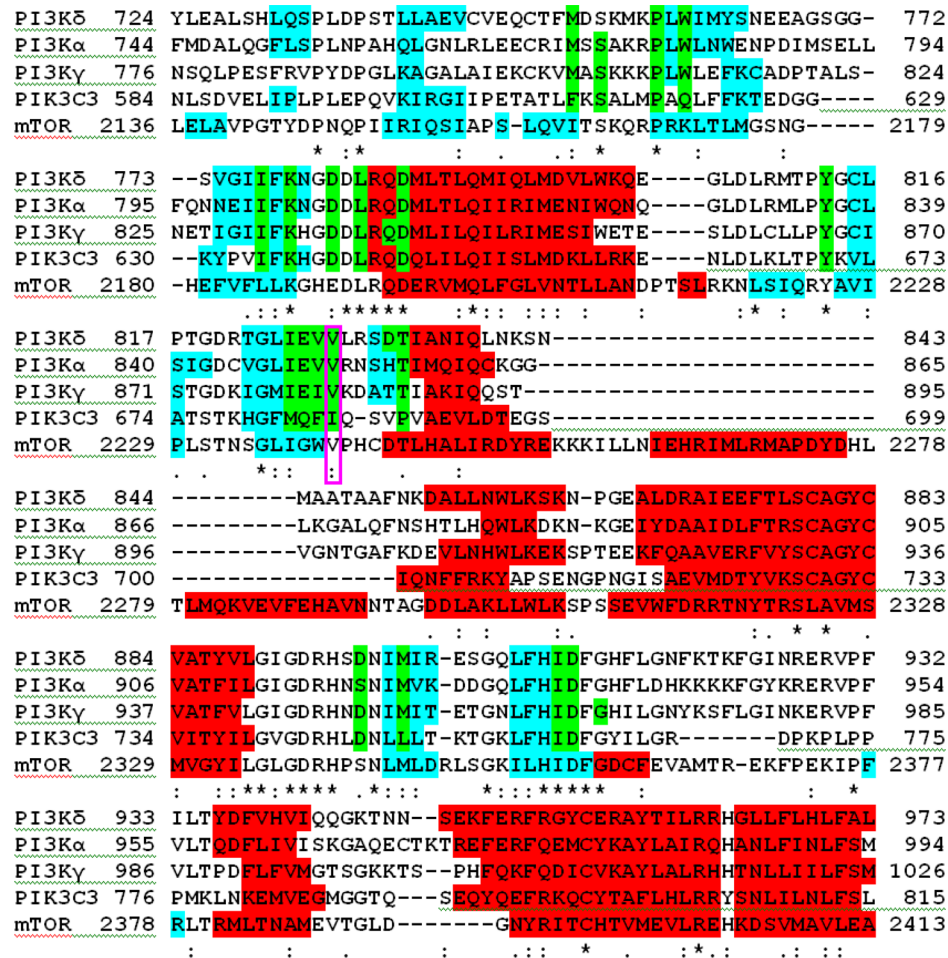


Figure 1. Alignment of the kinase domain of mTOR, PI3K α , PI3K δ , PI3K γ , and PIK3C3. Red: α helix; Blue: β strand, Green: ATP-binding site. Secondary structure information was taken from the X-ray structures for PI3K α , PI3K δ , PI3K γ , and PIK3C3 whereas it was calculated for mTOR. The magenta rectangle marks the residue used for hydrogen bond constraint during docking.

2. METHODS

2.1. Conformational Search, Force Fields, and Solvation Model. The molecules were built using Maestro 9.0⁶ or converted to 3D structures from the 2D structure using LigPrep version 2.3.⁶ Basic amines were protonated as in aqueous solution at physiological pH. The conformational space was searched using the Monte Carlo Multiple Minimum (MCMM) method⁷ as implemented in MacroModel version 9.7.⁶ All heavy atoms and hydrogens on heteroatoms were included in the test for duplicate conformations. All rotatable single bonds were included in the conformational search, and all aliphatic rings were ring-opened and quaternary atoms were allowed to invert. Each search was continued until the global energy minima were found at least 3 times. The energy minimizations were carried out using the truncated Newton conjugate gradient algorithm (TNCG) and the OPLS-AA force field^{8,9} as implemented in MacroModel. Default parameters were used. The conformational searches were done for aqueous solution using the generalized Born/solvent accessible surface (GB/SA) continuum solvation model.^{10,11}

2.2. X-ray Structures and Docking. The PI3K γ (entry 1E7V¹²), PI3K α (entry 2RD0¹³), PI3K δ (entry 2WXP¹⁴), and PIK3C3 (entry 3LS8¹⁵) X-ray structures were accessed from the Protein Data Bank (PDB).¹⁶ The protein structures, including the mTOR homology model (*vide infra*), were

prepared using the protein preparation wizard in Maestro with standard settings except that all water molecules were removed from the proteins. Grids were generated using Glide version 5.5⁶ following the standard procedure recommended by Schrödinger. A hydrogen bond constraint was included in the grid files. The backbone NH of the residue Val851 (PI3K α), Val882 (PI3K γ), Val828 (PI3K δ), Ile785 (PIK3C3), and Val2240 (mTOR) was forced to form a hydrogen bond to the morpholine oxygen of the ligand. This is the hydrogen bond donor in the hinge region of the kinase to which the 1-position of the purine of ATP forms a hydrogen bond. These residues are marked with a magenta rectangle in Figure 1. The compounds were docked using Glide with standard settings in both standard and extra precision mode. The docked poses discussed in this paper were not necessarily the highest scoring but were selected as the highest scoring pose with a reasonable conformation and binding mode as judged by the modeler.

2.3. Calculation of the Conformational Energy Penalty. The docked conformation was minimized with MacroModel using flat bottom Cartesian constraint with a half width of 1.0 Å and the default restraining force constant of 100 kJ/mol. This allows the docked conformations to relax (adjust) to the OPLS-AA force field.^{8,9} Without the relaxation the energy calculated by OPLS-AA would be grossly overestimated. This relaxation does not change the conformation as RMS between the docked and relaxed structures are <0.1 Å.

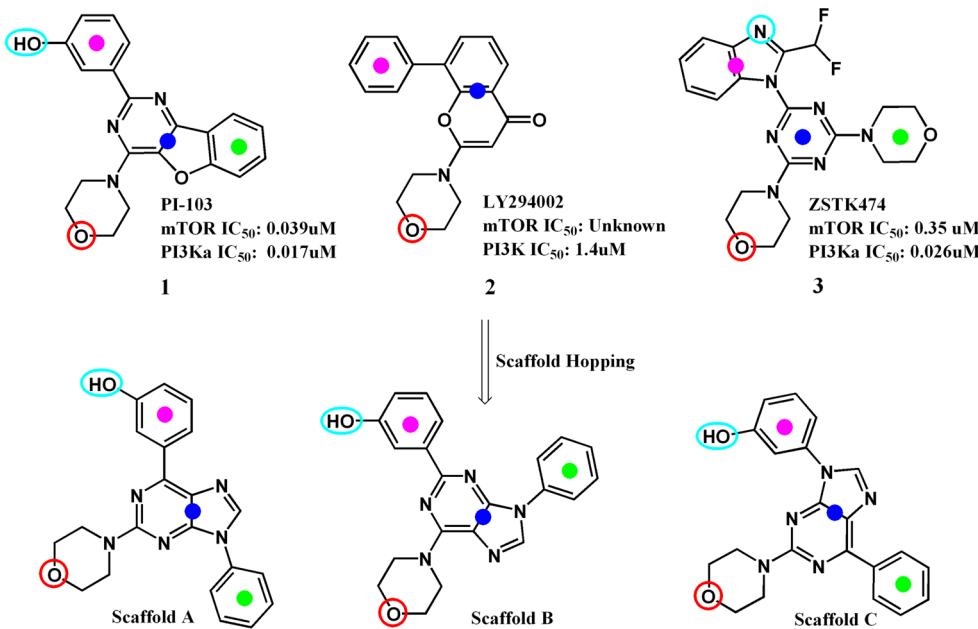


Figure 2. Reference compounds 1–3 (top) and proposed scaffolds A–C (bottom). The PI3K activity for LY294002 was taken from ref 29. The perceived pharmacophore elements are color coded. Hydrogen bond donor and acceptor atoms are circled, and hydrophobic groups are marked with centroids.

The conformational energy penalty of the docked conformations was calculated by subtracting the internal (steric) energy of the preferred conformation in aqueous solution (i.e., the energy of the global energy minimum in solution excluding the hydration energy) from the calculated energy of the docked conformation. Since the conformational ensemble was represented by only the global energy minima, entropy effects have not been taken into account. For flexible molecules this leads to an underestimation of the energy penalty. A limit of 3 kcal/mol (12.6 kJ/mol) for acceptable energy penalties was imposed as recommended by Boström et al.¹⁷

2.4. Homology Modeling. A homology model was build for mTOR. The protein sequences were downloaded from UniProt (accession numbers mTOR: P42345; PI3K α : P42336; PI3K γ : P48736; PI3K δ : O00329; and PIK3C3: Q8NEB9).¹⁸ The kinase domains were aligned using clustal W 1.83¹⁹ and then manually edited. The sequence identity for the alignment of mTOR kinase domain to the sequence of the X-ray structures (*vide supra*) of PI3K δ , PIK3C3, PI3K α , and PI3K γ , respectively is 28%, 26%, 24%, and 23%. The sequence identity and homology of binding site residues between mTOR and PI3K α is 63% and 79%, respectively. The secondary structure information was taken from the X-ray structures with the exception of mTOR where it was predicted by Psipred²⁰ and SSPPro.²¹ The alignment and secondary structure prediction is shown in Figure 1. The PI3K-alpha X-ray structure was used as a template. The homology models were build using Prime version 2.1⁶ with standard settings. Loops were not optimized. The homology model was finally subjected to 500 steps of Polak-Ribier Conjugate Gradient (PRCG) minimization using MacroModel⁶ with OPLS-AA force field⁹ and the GB/SA solvation model.¹¹ A number of mTOR X-ray structure has since been published.²² The mTOR modeling for this paper was redone using the X-ray structure 4JT6 which is also used for illustrations. RMSD between the HM and 4JT6 is 2.5 and 0.7 Å for superimposition of alpha carbons of binding site

residues. Use of the X-ray structure did not lead us to change any conclusions reached from use of the homology model.

2.5. DFT Calculations. The program Jaguar version 7.6⁶ was used for B3LYP DFT energy minimization. The chosen basis set was 6-31G**. The PBF²³ solvation model was used with water as solvent. Accuracy level was set to “Accurate” and grid density was set to “Fine”; otherwise default parameters were used. DFT calculations were done on fragments rather than whole molecules. These fragments consisted of the headgroup, the purine core with a methyl in the 9-position.

2.6. Compound Synthesis. All compounds (except when indicated) were synthesized by the chemistry department of SBIO Pte Ltd. The synthesis is described in the patent application WO/2009/045174.²⁴

2.7. In Vitro Kinase Assays. The recombinant enzymes (mTOR and PI3K-alpha) were generated by the Protein Biochemistry Group in S*BIO. Compounds were dose-titrated in 8 concentrations (3-fold serial dilution from the highest concentration of 50 μM for PI3K α , 4-fold serial dilution from the highest concentration of 20 μM for mTOR). IC₅₀ values were calculated from raw data using PRISM 5.²⁵

The routine assays with purified recombinant mTOR were performed in 384-well plates as follows. Enzyme and substrate (4eBP1)²⁶ were diluted in Kinase Assay Buffer (10 mM Hepes pH 7.5, 50 mM NaCl, 10 mM MgCl₂) to make a 2x enzyme–substrate premix. Separately, cold ATP and γ -³³P-ATP was also diluted in Kinase Assay Buffer to make a 2x ATP stock. To each well containing test compound in 1 μL of DMSO, 10 μL of the 2x enzyme–substrate premix was added, followed by 10 μL of the 2x ATP stock. The final reaction volume of 21 μL contained 2 μg/mL mTOR, 100 μg/mL of 4eBP1, 10 μM cold ATP, and 0.5 μCi γ -³³P-ATP (PerkinElmer). The reaction plate was incubated for 1 h at RT with gentle shaking and then terminated by adding 40 μL Stop Solution (20 mM EDTA and 1 mM cold ATP). 50 μL of the terminated kinase reaction mixture was transferred to a 384-well MultiScreen HTS-PH plate (Millipore Cat# MZPHNOW50) containing 50 μL of 1%

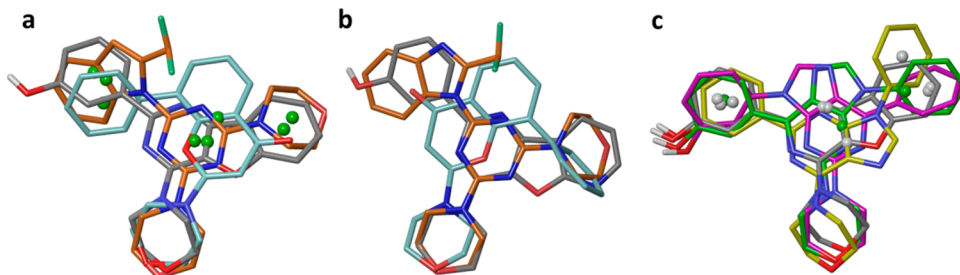


Figure 3. **a:** Superimposition of proposed reference compounds based on the pharmacophore hypothesis. The pharmacophore elements marked in Figure 2 were used as fitting points. PI-103 with gray carbon, LY294002 with cyan carbon, ZSTK474 with orange carbon. **b:** Overlay of compounds 1–3 from X-ray structures 1E7V, 2WXL, and 4L23 obtained from superimposition of binding site alpha carbons. **c:** Superimposition of scaffolds A–C on 1. Scaffold A with green carbon, scaffold B with yellow carbon, and scaffold C with magenta carbon. Centroids are shown as white spheres.

phosphoric acid and incubated for 15 min. The wells were then drawn through a vacuum and washed four times with 120 μ L of 0.5% phosphoric acid. The base was sealed, and 10 μ L of BetaPlate scintillation cocktail (Cat#1205-440, PerkinElmer) was added to each well. The top was sealed, and the plates were read on the Wallac Microbeta counter (PerkinElmer).

The routine assays with purified recombinant PI3K α (p110 α /p85) were performed in 384-well format as follows. Substrates²⁷ phosphatidyl inositol (Sigma-Aldrich Cat#P2517) and phosphatidyl serine (Sigma-Aldrich Cat#P5660) (1:1 at 0.1 mg/mL each, 20 μ L per well) were used to coat a 384-well Maxisorp plate (Nunc Cat#460372) by overnight evaporation in a fumehood. Enzyme, ATP and test compound are then added to the dried coated wells to give a final reaction volume of 25 μ L containing 0.2 μ g/mL p110 α /p85 complex, 2 μ M cold ATP, 0.05 μ Ci γ -³³P-ATP, and a desired concentration of test compound per well in Assay Kinase Buffer (100 mM Tris-HCl pH 7.0, 200 mM NaCl, 8 mM MgCl₂). The reaction plate was incubated for 1 h at RT with gentle shaking and then terminated by adding 30 μ L of Stop Solution (50 mM EDTA, pH 8.0). The wells were then washed two times with 90 μ L of TBS pH 8.0 and dried under the fumehood for at least 1 h. Thirty μ L of Optiphase “SuperMix” scintillation cocktail (Cat#1200-439, PerkinElmer) was added to each well. After 1 h incubation, the plates were sealed and read on the Wallac Microbeta counter (PerkinElmer).

3. RESULTS AND DISCUSSION

3.1. Background. A literature search revealed several PI3K inhibitors based on a variety of scaffolds (Figure 2). Compound **1** (PI-103) is a potent dual PI3/mTOR kinase inhibitor developed by Astellas Pharma.²⁸ **2** (LY294002) is a moderately active PI3 kinase inhibitor published by Eli Lilly,²⁹ while **3** (ZSTK474) is a potent PI3/mTOR inhibitor with 10-fold selectivity for PI3K. This compound was developed by The Japanese Foundation for Cancer Research.³⁰ These inhibitors were found to have distinct groups in common leading us to believe they shared the same binding-mode. These pharmacophore elements are shown in Figure 2: (i) A central core consisting of an aromatic ring system marked with a blue centroid. (ii) A second binding motif, referred to as the headgroup, is marked with a magenta centroid. This group may incorporate hydrogen bond donor and acceptor atoms that are circled in cyan. (iii) A hydrophobic group marked with a green centroid. (iv) The morpholine group with its oxygen atom as a hydrogen bond acceptor is circled in red. A superimposition of the 3D structures of compounds **1–3** confirmed that the pharmacophore elements overlap in space (Figure 3a). X-ray

structures of compounds **2** (PI3K γ with LY294002, PDB-ID 1E7V),¹² compound **3** (PI3K δ with ZSTK474, PDB-ID 2WXL),¹⁴ and with **1** (PI3K α with PI-103, PDB-ID 4L23)³¹ have been published subsequently confirming this binding hypothesis except that the phenyl of **2** superimpose with the hydrophobe and not the headgroup (Figure 2b). However, a class III PI3K X-ray structure with **1** (PDB-ID 2X6K)³² has the alternative rotamer for the phenol compared to that of 4L23 indicating that either there is little difference in the interaction energy between the two rotamers and/or that the orientation of the phenol may be used to obtain PI3K subtypes selectivity.

3.2. Scaffold Hopping. We designed three scaffolds A–C having a purine core that were substituted with a morpholine, a phenol headgroup, and a hydrophobic substituent. These are shown with their pharmacophore elements marked in Figure 2, bottom. Figure 3c shows a superimposition of the designed scaffolds onto the reference compound **1**. It was not immediately obvious which scaffold was the best choice as **1** superimposed best on scaffold A, **2** superimposed best on scaffold C, and **3** superimposed best on scaffold B. However, scaffold A is best contained within the common volume of the reference compounds **1–3**. This was in line with our medicinal chemists who prioritized this scaffold for synthetic reasons. Figure 4 defines substituents of the purine core for the selected

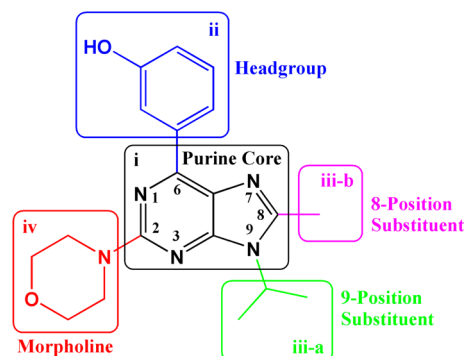


Figure 4. Definition of the names of substituents connected to the purine core. We selected the purine scaffold A in Figure 2.

scaffold and its pharmacophore elements. Notice that pharmacophore element (iii) may be accessible from both the 8- and 9-positions of the purine scaffold.

3.3. Lead Optimization of Headgroup. During lead identification and early optimization work compounds were prepared via a general three step synthetic route starting from readily available 2,6-dichloropurine. Elaboration involved initial

functionalization of the 9-position of the purine scaffold. Coupling to an aromatic group at the 9-position proved synthetically challenging, while aliphatic substituents were more easily introduced. Compound 4 with a 9-position benzyl was the first compound synthesized (Table 1). 4 has a MW of 387

Table 1. SAR of Headgroups^c

Cpd	Headgroup	mTOR IC ₅₀	PI3 α IC ₅₀	Cpd	Headgroup	mTOR IC ₅₀	PI3 α IC ₅₀
4		0.4	0.089	12		0.11	0.017
5		>10	>10	13		0.16	0.12
6		2.1	0.13	14		4.0	0.18
7		>10	>10	15		1.6	1.6
8		9.4	NT	16		0.42	0.076
9		7.3	0.69	17		3.3	0.59
10		1.4	>10	18		0.39	0.095
11		0.30	0.034	19 ^a		0.087	0.075

^aThe 9-position side chain is 3-pentyl. NT is not tested. ^bAn asterisk denotes the attachment point. ^cActivities in μM are the mean of at least 2 experiments.

Da, an inhibitory activity of $0.40 \mu\text{M}$, and $0.089 \mu\text{M}$ for mTOR and PI3 α , respectively, corresponding to a LE (ligand efficiency) of 0.30 and 0.33 kCal/mol/HA, respectively. This was judged to be an excellent starting point for lead optimization. Figure 5 shows compound 4 docked into PI3 α . The purine core has hydrophobic contact with the side chains of Ile800, Met922, and Ile932. The morpholine group hydrogen bonds to the backbone NH of the kinase hinge residue Val851 and has hydrophobic contacts with the side chains of Trp780, Ile800, Tyr836, Val851, Met922, Phe930, and Ile932 and the gatekeeper residue Ile848. The benzyl group has hydrophobic contacts with the side chains of Met772, Thr856, and Met922. The hydroxyl of the phenol headgroup hydrogen bonds to Tyr836 and Asp810, while the aromatic ring has hydrophobic contacts with the side chains of Ile848, Ile932, and Asp933 as well as the α carbon of Asp933. An additional electrostatic interaction may be associated with the backbone NH of Asp933 which points toward the carbon bearing the hydroxyl functionality of the phenol. The angle between the plane of the phenol ring and the vector of this interaction is 92° . A comparison to the recently published PI3 α structure with 1 shows essentially identical binding mode for the phenol. The morpholine and tricyclic core of 1 has very similar hydrophobic interactions as those described for 4.³¹ A close-up of the headgroup of 4 docked into PI3 α is shown in Figure 6a. The donor, and to a lesser extent acceptor, functionality of the phenol was thought to be important for binding (compare to 5), and it was believed activity could not be improved much by optimizing this position. However, the headgroup of 4 was thought to be a liability due to its potential to be rapidly metabolized. Phenols are known to react with glucoronic acid *in vivo*, and the conjugate is rapidly excreted thereby compromising bioavailability. This prompted us to search for a bioisosteric replacement of the headgroup, i.e. a group that contained both an aromatic ring as well as hydrogen bond donor and acceptor atoms.

The benzylic alcohol of 6 is an obvious replacement. This group is slightly larger than the phenol, but when docked into PI3 α it still forms the same hydrogen bonds as that of 4. This is shown in Figure 6b. In the PI3K γ X-ray structure 3L13³³ the 4-morpholine-thienopyrimidine ligand has a benzylalcohol headgroup like 6. In this structure the hydroxyl group hydrogen bonds with both the tyrosine and aspartic acid, but an

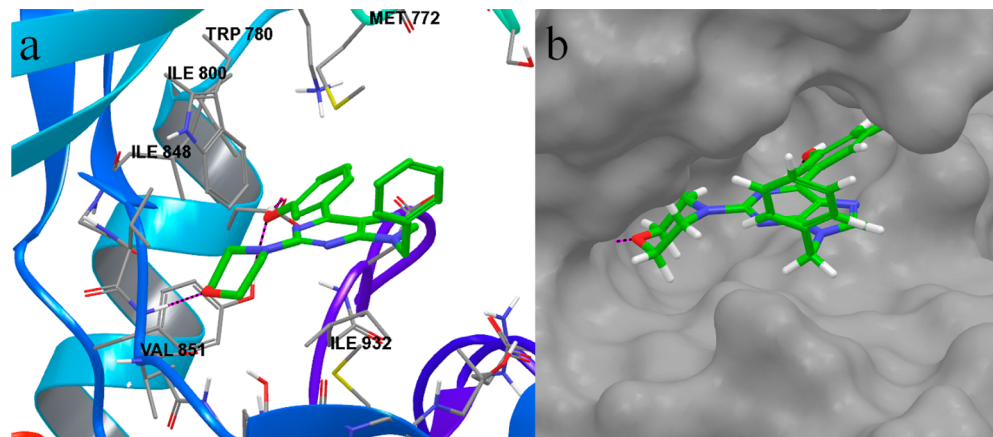


Figure 5. a: Compound 4 docked into the ATP-binding site of PI3 α . 4 is shown as a thick tube with green carbon, while the protein is shown as a thin tube with gray carbon. Hydrogen bonds between the protein and inhibitor are shown in magenta/black dashed lines. b: PI3 α is shown as a gray surface. The bulge in the bottom of the binding site is Gln859.

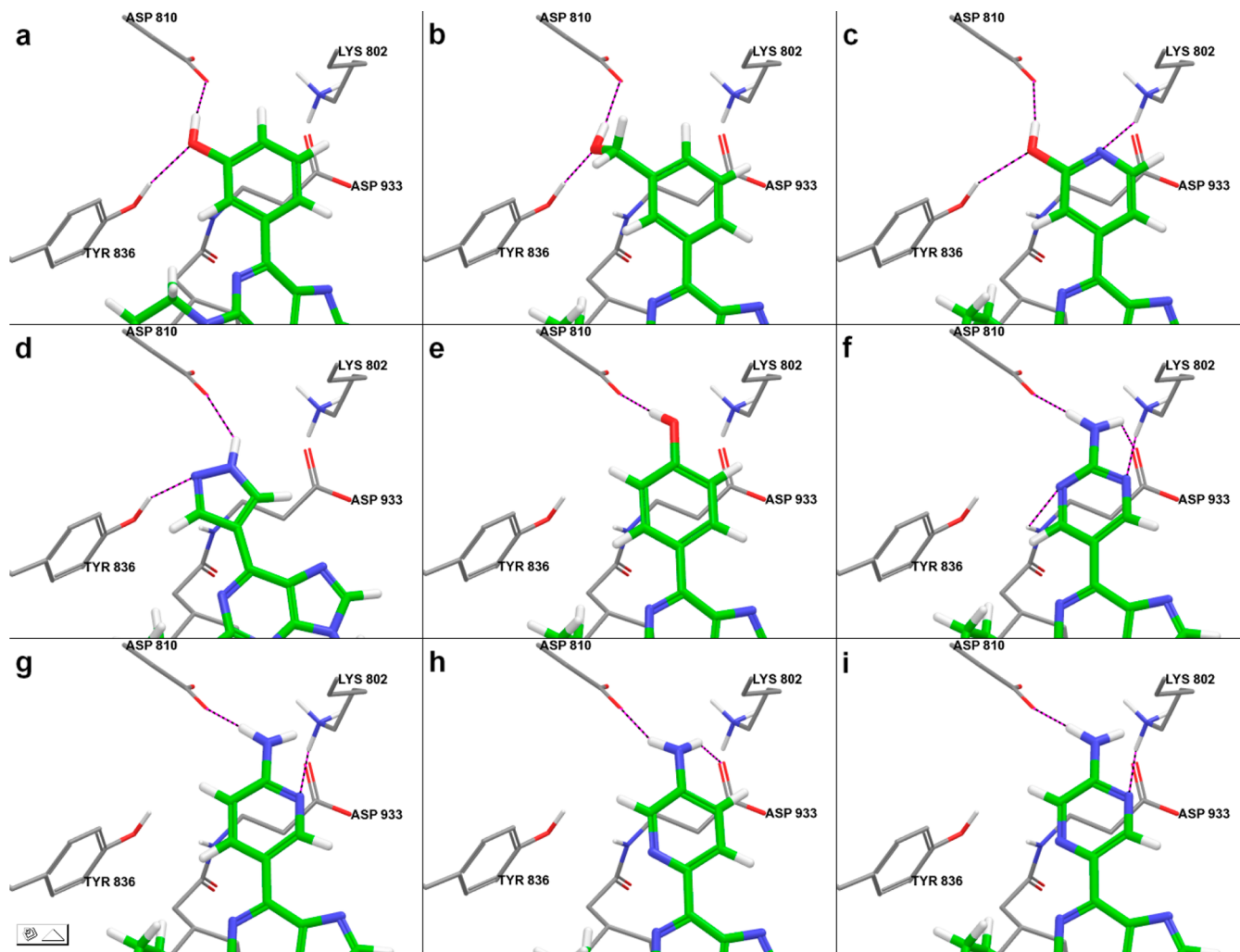


Figure 6. Optimization of headgroups. Compounds **4**, **6**, **7**, **9**, **10**, **11**, **13**, **15**, and **19** docked into PI3K α . Only the area around the headgroup is displayed. The observed hydrogen bonding pattern explained the relative potencies of the different headgroups.

additional probably weak hydrogen bond to the NH backbone of Asp964 is observed (distance between heavy atoms is 3.2 Å). While the PI3K α activity of **6** is on par with that of **4**, the mTOR activity decreased 4-fold. Furthermore, a benzylic alcohol still constitutes a potential metabolic liability through rapid oxidation by cytochrome P450 enzymes. The aza-phenol **7** docks into PI3K α in a similar fashion to **4**, and the nitrogen may form a hydrogen bond to the catalytic lysine Lys802 (Figure 6c). However, **7** was found to be a poor inhibitor of mTOR and PI3K α . This is probably due to the pyridone tautomer of **7** being the dominant species in aqueous solution. DFT B3LYP/631G** calculations reveal that this tautomer is 20 kJ/mol lower in energy than the aza-phenol. Using eq 1 and assuming all else being equal, a $\Delta\Delta G$ of 20 kJ/mol corresponds to a ΔK_i of more than 3000. The energetically favored pyridone tautomer does not dock well into PI3K α as the interaction between the pyridone-oxygen and Asp810 as well as that of the NH donor and the catalytic lysine Lys802 are both repulsive. The phenyl-amide **8** is a more bulky phenol bioisostere with both donor and acceptor functionalities pointing in the desired directions. However, **8** showed a marked drop off in enzymatic activity. Indeed this analogue could not be docked into PI3K α due to the amide clashing with the protein.

$$\Delta G = RT^*\ln[K_d] \sim RT^*\ln[IC_{50}] \quad (1)$$

17

Compound **9** could be docked into PI3K α forming hydrogen bonds to both Asp810 and Tyr836 (Figure 6d). However, this headgroup is smaller than phenol, and, in order to form these hydrogen bonds, the purine core is rotated in the binding site decreasing hydrophobic contacts and resulting in a steric clash between the morpholine and the protein.

Similarly to the *meta*-substituted phenol **4**, the *para* analogue **10** forms a hydrogen bond to Asp810; however, the hydroxyl is now no longer in a position to hydrogen bond to Tyr836, and the hydroxyl-oxygen may have an unfavorable interaction with Asp933 (Figure 6e) thereby explaining the lower affinity of **9** compared to **4**. While **10** is devoid of PI3K α activity it has an mTOR IC₅₀ of 1.4 μ M. The docked pose of **10** suggests that a NH₂ group in the *para* position should be able to favorably interact with both Asp810 and Asp933. The first compound prepared bearing a *para*-NH₂ was the aminopyrimidine **11** which is displayed in Figure 6f. The amino group forms the two hydrogen bonds to the aspartic acids, while the pyrimidine nitrogens form additional hydrogen bonds with the backbone NH of Asp933 and the catalytic lysine Lys802. In the PI3K γ X-ray structure 3APD³⁴ the ligand is a dihydro-pyrrolo-pyrimidine analogue of **11** with a morpholine and aminopyrimidine headgroup. The headgroup hydrogen bonds to Asp836 and the

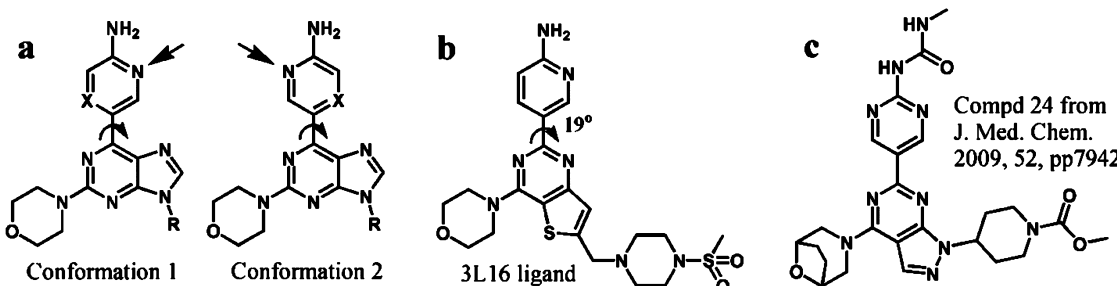


Figure 7. **a:** Compounds with an aminopyrazine or aminopyridine headgroup may bind with different orientations of the aromatic ring. The conformational energy difference is calculated by DFT B3LYP/6-31G** to be less than 1 kJ/mol for both headgroups. The torsional angle discussed in the text is marked with a bend arrow. The hydrogen bond donor interaction is marked with a straight arrow. **b:** The structure of the cocrystallized ligand in the PDB structure 3L16.³³ The orientation of the aminopyridine headgroup is that of conformation 1. **c:** This bridged morpholine compound was reported to be 1800-fold selective toward mTOR.³⁵ The compounds shown in parts **b** and **c** were not synthesized in SBIO Pte Ltd.

catalytic lysine, but the distance to the backbone NH of Asp964 is too big for hydrogen bonding and the geometry does not allow hydrogen bonding to the side chain of Asp964 although the distance to the headgroup NH₂ is 3.0 Å. The aminopyrimidine headgroup was found to be equipotent with the phenol in inhibiting mTOR but had a 3-fold greater inhibitory activity toward PI3K α . While the aminopyrimidine headgroup solved the metabolic liability, it introduced an imbalance in the inhibitory activity between mTOR and PI3K α being 10 times more potent toward PI3K α . Further kinase profiling of **12** found that the compound was inhibiting all the class I PI3K isoforms. The putative binding modes were almost identical to that of PI3K α when docked into PI3K δ and PI3K γ .

Further optimization of the headgroup did not improve inhibitory activity; however, a number of observations were made that subsequently aided optimization of mTOR selectivity. Figure 6g shows compound **13** with an aminopyridine headgroup docked into PI3K α . Having one acceptor less than **12**, compound **13** forms one less hydrogen bond to the protein. This has a much larger effect on the PI3K α activity which drop 7-fold compared to the much smaller drop in mTOR activity of 1.5. This suggests that both pyrimidine nitrogens are important for PI3K α binding, while only one of them forms a good hydrogen bond interaction in mTOR. This would explain why the aminopyrimidine is selective toward PI3K α over mTOR, while the aminopyridine is equipotent.

Compound **14** contains the pyrimidine headgroup but lacks the amino substituent and is thus unable to form the two hydrogen bonds to Asp810 and Asp933. This is in keeping with the observed inhibitory activities which is a factor of 11 and 36 less for PI3K α and mTOR, respectively, than for compound **12**. **15** is an isomer of **13** with the pyridine nitrogen in the *meta* position to the amine. In the docked pose of **15** this nitrogen does not form any hydrogen bonds to PI3K α (Figure 6h). This compound also shows a 94-fold decrease in mTOR activity and a 15-fold drop off for PI3K α with respect to **12**. The methylamide **16** and sulfonamide **17** supported the observation from the docked pose of **11–13** that both hydrogen bond donors of the aminopyrimidine headgroup are important for activity. Compound **16** may be docked into both PI3K α and mTOR, whereas the methylsulfonyl of **17** is seen to clash with residues in both proteins. Based on the observations drawn from compounds **11–18** we concluded that an aminopyrazine headgroup should be potent and have a good balance between PI3K and mTOR inhibition. Compound **19** having this headgroup is shown in Figure 6i. While the inhibitory activity was 4-fold less toward PI3K α than **12**, the mTOR activity was

the same as for **12** resulting in equipotent inhibition of the two proteins.

While the aminopyrimidine headgroup has rotational symmetry the aminopyrazine or aminopyridine do not, leading to two possible binding modes that differ only by the orientation of the headgroup as shown in Figure 7. The energy difference between these conformations is negligible as calculated by DFT B3LYP/6-31G** (less than 1 kJ/mol for both headgroups), so the conformational energy penalty may not rule either of them out (eq 1). When docked into PI3K α the preferred pose is conformation 1 for both the aminopyrazine and aminopyridine headgroup. The aromatic nitrogen forming a hydrogen bond to the protein is marked with an arrow in Figure 7. Conformation 1 hydrogen bonds with the catalytic lysine Lys802 (6G and 6I), whereas conformation 2 hydrogen bonds with the NH backbone of Asp933. To form a hydrogen bond with a favorable geometry to Lys802 the torsional angle between the purine core and the headgroup in conformation 1 should be between 0° and 35°. For conformation 2 this angle needs to be 40–80° in order to form a hydrogen bond with good geometry to the NH backbone of Asp933. The torsional angle in the force field minimized conformations of the purine-aminopyrimidine is ~35° for both conformations, whereas it is 33° and 18° for conformations 1 and 2 of the purine-aminopyrazine. This does not rule either conformation out; however, the DFT minima of both conformations of both headgroups are flat which supports conformation 1 as the bioactive conformation. Recently a PI3K γ X-ray structure cocrystallized with a small molecule inhibitor having a fused thienepyrimidine core, a morpholine hinge binder, and an aminopyridine headgroup with a geometry similar to **1** have been published (Figure 7b).^{14,33} This inhibitor has the pyridine nitrogen pointing toward Lys802, and the torsional angle between the core and headgroup is 19°. The electron density of this structure is not high enough to determine the difference between carbon and nitrogen, so the experimental evidence neither supports nor disproves our conclusion that conformation 1 is the bioactive conformation of the aminopyridine and aminopyrazine headgroups. When docked into mTOR conformation 2 is the preferred conformation for pyrazine headgroups (*vide infra*) so different orientation of the pyrazine may explain the selectivity difference for compounds having this headgroup.

3.4. Optimization of 9-Position Side Chains. In parallel with the headgroup optimization, compounds with various 9-position substituents were synthesized with the aim of improving inhibitory potency mainly toward mTOR (Table

2). Compounds **20** and **21** are derivatives of **4** with fluorine substituents on the benzyl side chain. These substituents

Table 2. SAR of the 9-Position Substituent^b

Cpd	Substituent	mTOR IC ₅₀		PI3 α IC ₅₀	
		Cpd	Substituent	mTOR IC ₅₀	PI3 α IC ₅₀
4	*-C ₆ H ₅	0.40	0.089	12	-CH ₂ CH ₃
20	*-C ₆ H ₄ F	0.17	0.13	29	*-C ₃ H ₅
21	*-C ₆ H ₄ F	0.18	0.14	30	*-C ₃ H ₇
22	*-CH ₂ O-	0.51	0.035	31	*-C ₃ H ₅ O-
23	*-CH=CH-	0.12	0.047	32	*-CH(CH ₃) ₂
24	*-C ₆ H ₅	0.057	0.85	33	*-C ₃ H ₅ NH-
25	*-C≡N	0.26	0.027	34	*-C ₆ H ₄ CH ₃
26	*-C ₆ H ₅	0.22	0.52	35	*-C ₆ H ₅
27	*-C ₃ H ₅	0.062	0.030	36	H
28	*-C ₃ H ₇	0.016	0.028	37	*-C ₆ H ₁₁

^aAn asterisk denotes the attachment point. ^bDual mTOR & PI3K inhibitors. Activities in μM are the mean of at least 2 experiments.

improved mTOR activity slightly through greater hydrophobic interaction with the protein, but PI3 α activity was not altered significantly. The 1-phenylethyl substituent of **26** also improved mTOR activity slightly but decreased PI3 α activity 6-fold inducing a degree of mTOR selectivity. When docked into mTOR the benzyl group is in a high energy conformation but has good hydrophobic contacts with the protein. When docked into PI3 α some poses show the benzyl in a low energy conformation that clashes with the protein but otherwise has few hydrophobic contacts with the protein. (Figure 5) Other poses have the benzyl in a high energy conformation with few contacts to the protein.

The isobutyl substituent of **12** (Figure 8a and b) improved activity toward both mTOR and PI3 α presumably by lowering the conformational energy penalty. Both the ether and the vinyl substituent of compounds **22** and **23** docked well into both proteins although with little hydrophobic contact in the case of PI3 α . The binding site around the 9-position in PI3 α is wider than that of mTOR, and larger substituents are required to make good contact with PI3 α . However, these side chains must also have some flexibility in order not to clash with Gln859. This may be the reason why we did not see much improvement in PI3 α activity beyond that of **12** during the course of optimization of the 9-position. Later compound **36** without a 9-position substituent were synthesized with a surprisingly high PI3 α activity but poor mTOR activity.

Interestingly **23** was 4 times more active against mTOR than **22** which docks into mTOR with the ether substituent in the same conformation as the alkene. This difference may be due to the higher lipophilicity of the 9-position substituent of **23**. The area in mTOR surrounding the 9-position is very hydrophobic with the side chains of Trp2239, Leu2163, and Leu2185 lining the edge of the binding site. This may explain mTOR's preference for lipophilic substituents here. A similar trend can be seen when comparing the mTOR activity of **28** and **30** to that of **31** to **33**. This may also be the reason for the PI3K selectivity of **25** despite the observed docking interaction of the cyano group with Trp2239 of mTOR.

We were interested in synthesizing a compound with a phenyl substituent directly attached to the 9-position due to the possible favorable interaction with Trp2239 in mTOR. Compound **24** and **35** are examples of these with **35** shown docked in Figure 8c and d. **35** has a good aromatic–aromatic interaction between Trp2239 of mTOR and the 9-position substituent. The equivalent residue in PI3 α is Val850 without any contacts to the substituent. The PI3 α has the phenyl in a low energy conformation without much interaction with the protein. Unfortunately directly attached aromatic 9-position substituents were challenging to synthesize as well as exhibiting poor aqueous solubility due to their flat aromatic nature. As a result this direction was not pursued further.

Certain compounds containing larger conformationally constrained side chains, such as **34** and **37**, showed surprisingly poor inhibition of PI3 α . Docking revealed that these bulkier side chains either clashed with the protein structure of PI3 α or were forced into a higher energy conformation with little contact to the protein. This is shown in Figure 8e for **37**. However, when docked into mTOR the same analogues adopted low conformational energy poses, and part of the side chain was able to access a small hydrophobic groove surrounded by the residues Trp2239, Leu2163, and Leu2185 (Figure 8f).

Correlation of the SAR between phenol substituted analogues and the aminopyrimidine headgroup series was not always observed. This can be seen when we compare the phenols **24** and **27** to the aminopyrimidines **35** and **29**. The 9-*meta*-methylphenyl side chain results in selectivity toward mTOR in the case of a phenol headgroup (**24**), but this selectivity is not observed for the corresponding aminopyrimidine (**35**). Similarly, the methylene-cyclopropyl side chain imparts potency against both proteins when phenol is the headgroup (**27**) but results in selectivity toward PI3 α with an aminopyrimidine headgroup (**29**). The different headgroups positions the purine scaffold slightly differently in the binding site. Therefore, the location and direction of the 9-position substituent within the kinase binding site will vary depending on the choice of headgroup. This may have profound effects on the kinase activity of compounds with bulky 9-position substituents.

3.5. Optimization of 8-Position Side Chains. The synthesis of compounds with substituents in the 8-position proved more challenging although a few were successfully prepared. Larger substituents, such as the phenyl in **41**, proved detrimental to PI3 α activity. When docked into PI3 α larger substituents would clash with the glycine rich loop. Larger substituents may also adversely affect binding as a result of their influence on the conformation of the 9-position substituent. In an energy minima, the hydrogen on the carbon connected to the 9-position of the purine, such as in **38** (Table 3), will lie in

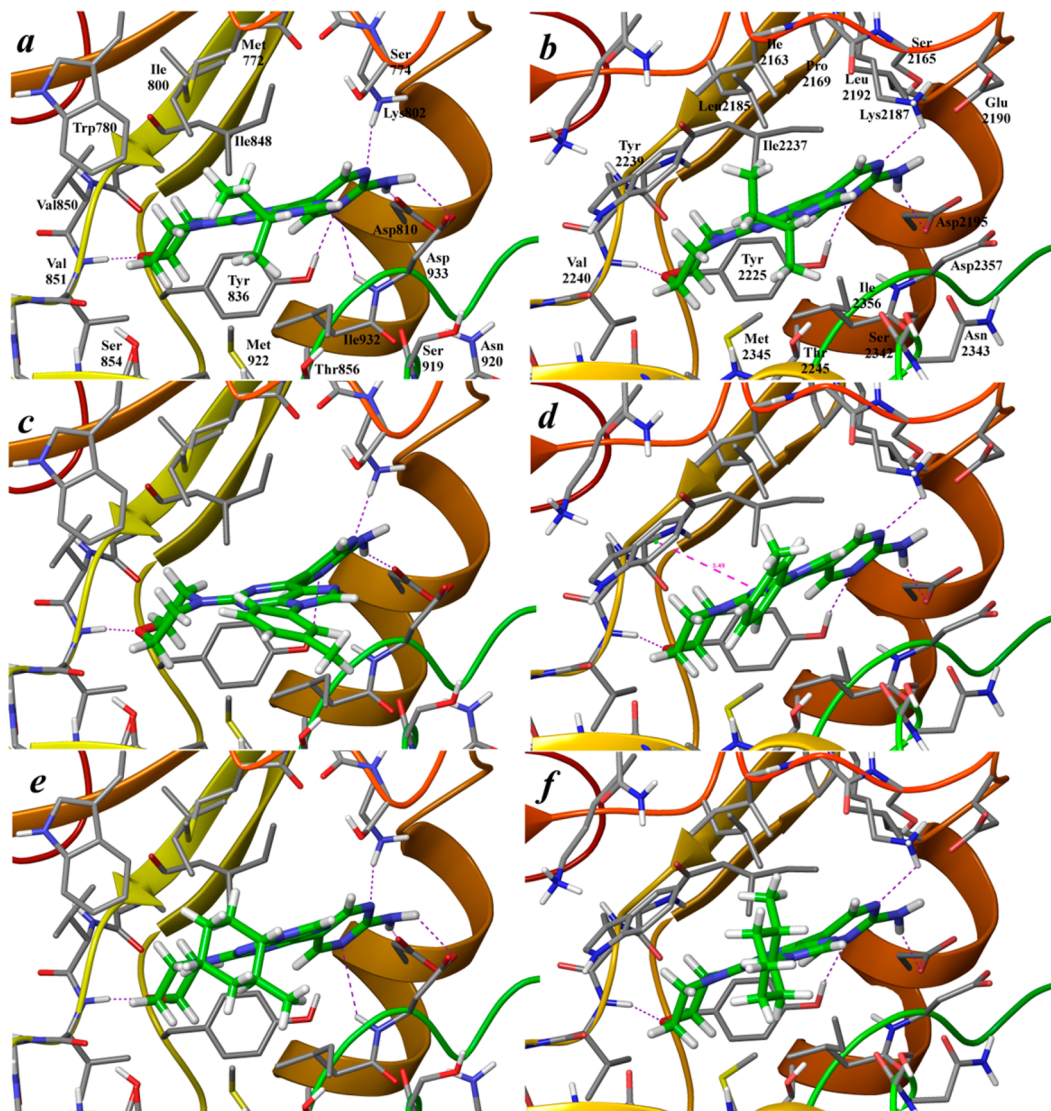


Figure 8. Optimization of 9-position side chains. Compounds **12** (a and b), **35** (c and d), and **37** (e and f) docked into PI3K α (left) and mTOR (right). While mTOR activity could be significantly improved, it was observed that some side chains reduced PI3 kinase activity. This was later used in our selective mTOR inhibitor project.

the plane of the purine ring, but it may adopt one of two opposing orientations, pointing toward or away from the 8-position. With no 8-position substituent, or with a small substituent, there is little conformational energy difference. With larger substituents in the 8-position there will be a preference of the 9-position substituent to point away from the 8-position.

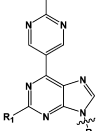
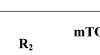
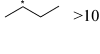
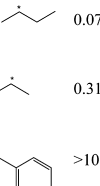
Smaller 8-position substituents increased activity through improved hydrophobic contacts with residues Ile2163, Ser2165, and Pro2169 in mTOR and Met772, Ser774, and Pro778 in PI3K α (Figure 9). The potent dual inhibitor SB2343 (compound **39**) with mTOR and PI3K α activities of 37 nM and 16 nM, respectively, was selected for further profiling and found to have excellent PK and ADME properties as well as being active in animal models.³⁶ With a molecular weight of 354 Da this is a small compound with high ligand efficiencies of 0.39 and 0.41 kCal/mol/HA for mTOR and PI3K α , respectively. SB2343 is being developed as VS-5584 and has recently entered phase I clinical development in a dose escalation study in subjects with advanced nonhematologic malignancies or lymphoma (NCT01991938).

3.6. Optimization of the Hinge Binder and mTOR Selectivity.

The morpholine oxygen forms a hydrogen bond to the backbone NH of the hinge residue Val2240 of mTOR. While this is essential for the kinase activity of our scaffold, morpholines are rare as hinge binders in protein kinase inhibitors. Having a morpholine hinge binder is thus an excellent way of achieving selectivity over other protein kinases. **45** has the morpholine substituted for the common protein kinase hinge binder aminopyrimidine, but it was found to be devoid of lipid kinase activity. The methylpiperazine **42** (Table 3) and other morpholine replacements (data not shown) proved to be devoid of kinase activity.

Compounds with substituents on the morpholine ring were generally less active while **43** was equipotent with **12**. The low energy conformation of **43** has the methyl in an axial conformation. This may be docked into mTOR without clashing with the protein, whereas compounds with substituents next to the morpholine oxygen only dock in high energy conformations as low energy conformations of these have the substituents equatorial. As early results were disappointing, we did little work on the morpholine until

Table 3. SAR of 8-Substituted Inhibitors (Left) and Morpholine Derivatives (Right)^b

Cpd	Substituent	mTOR IC ₅₀		PI3 α IC ₅₀		Cpd	Substituents	R ₁	R ₂	mTOR IC ₅₀		PI3 α IC ₅₀	
		mTOR IC ₅₀	PI3 α IC ₅₀	mTOR IC ₅₀	PI3 α IC ₅₀					mTOR IC ₅₀	PI3 α IC ₅₀	mTOR IC ₅₀	PI3 α IC ₅₀
38	H	0.15	0.017	42		>10	>10						
39	SB2343	Me	0.037	0.016	43		0.071	0.011					
VS-5584					44		0.31	0.25					
40	Br	0.018	0.018	45		>10	>10						
41	Ph	0.13	0.13										

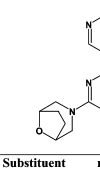
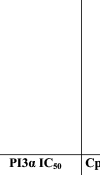
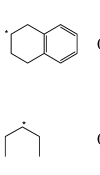
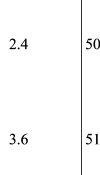
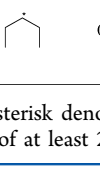
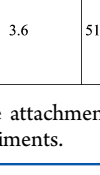
^aAn asterisk denotes the attachment point. ^bActivities in μM are the mean of at least 2 experiments.

pyrazolopyrimidine inhibitors with a bridged morpholine (Figure 7c) were reported to be selective mTOR inhibitors.³⁵ We decided to synthesize a purine compound with a bridged morpholine in combination with an aminopyrimidine headgroup. However, this compound was somewhat less active than the unsubstituted morpholine on mTOR and much less active on PI3K α (compare 44 to 38). Compounds with a bridged morpholine docked well into mTOR but clashed with Phe930 when docked into PI3K α . The equivalent residue in mTOR is the smaller Leu2354.

Compounds 19 and 44 are both equipotent mTOR and PI3K α inhibitors. When the bridged morpholine and aminopyrimidine headgroup were combined, it was observed that PI3K α activity was much reduced while maintaining mTOR activity. In 46–48 (Table 4) the bridged morpholine and aminopyrimidine headgroup were combined with a 9-position substituent that we had previously found to be mTOR selective. The resulting compounds have selectivity of up to more than 100-fold toward mTOR. Figure 10 show 48 docked into mTOR.

With a molecular weight of 394 Da 48 (SB2602) is a relatively small compound with high ligand efficiency for mTOR of 0.35 kCal/mol/HA. SB2602 is potent and 110-fold

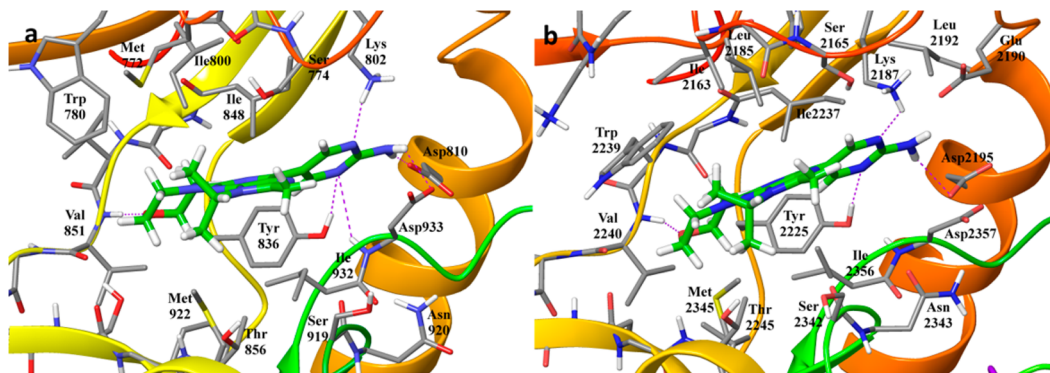
Table 4. SAR of mTOR Selective Compounds with Bridged Morpholine and an Aminopyrimidine Headgroup (Left) and Various Scaffold Derivatives (Right)^b

Cpd	Substituent	mTOR IC ₅₀		PI3 α IC ₅₀		Cpd	Scaffold	mTOR IC ₅₀		PI3 α IC ₅₀	
		mTOR IC ₅₀	PI3 α IC ₅₀	mTOR IC ₅₀	PI3 α IC ₅₀			mTOR IC ₅₀	PI3 α IC ₅₀	mTOR IC ₅₀	PI3 α IC ₅₀
46		0.12	4.4	49		2.1	0.051				
47		0.032	2.4	50		>10	0.070				
48		0.033	3.6	51		0.34	0.0023				

^aAn asterisk denotes the attachment point. ^bActivities in μM are the mean of at least 2 experiments.

selective for mTOR with an IC₅₀ of 33 nM. Further profiling found the compound to have good PK and ADME properties as well as activity in xenograft models. This compound was selected for preclinical development.

3.7. Comparison of Various Scaffolds. During the project a few other scaffolds and various changes to the purine core were explored. The 7-position nitrogen of the purine was replaced by a carbon atom in 49 (Table 4). This resulted in a dramatic loss of mTOR activity and a smaller loss of PI3K α activity (compare to 12). DFT minimization indicates that the headgroup is coplanar with the purine in 12, while the torsion is 24° in the energy minima of 49. The energy difference between the minima and the conformation with a coplanar headgroup is 3.8 kJ/mol calculated by DFT. This corresponds to a 5-fold decrease in activity using eq 1 which is in keeping with the observed activity for PI3K α but may not fully explain the large drop in activity for mTOR. Another explanation for the loss of mTOR activity of 47 could be that the 7-position nitrogen in the purine scaffold hydrogen bonds to the catalytic lysine Lys2187 either directly or through a water molecule. When docked into mTOR, there is enough space between the 7-position of compound 12 and Lys2187 to accommodate a

**Figure 9.** Compound 39 (SB2343, VS5584) docked into PI3K α left and mTOR right. Small substituents in the purine 8-position increased activity toward both mTOR and PI3K α .

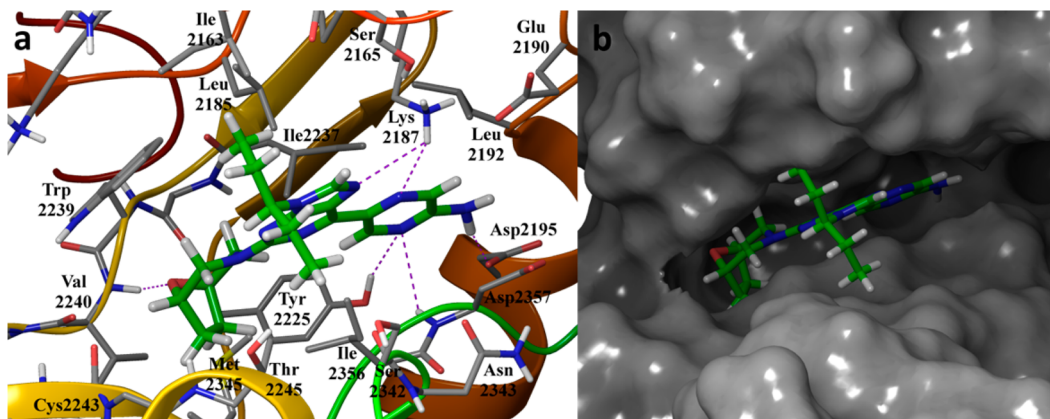


Figure 10. Compound 48 (SB2602) docked into mTOR. **a:** Protein shown as cartoon with binding-site residues in gray carbon. **b:** mTOR shown as gray surface. The combination of an aminopyrazine headgroup with a bridged morpholine resulted in potent and selective mTOR inhibitors. This compound did not dock well into PI3K α .

water molecule. The same reasoning may explain the dramatic reduction observed for tetrahydropyridopyrimidine **50**. In this case the torsion between the purine and headgroup is 33° in the DFT minima, and the energy difference between that and the conformation with the headgroup in the scaffold plane is 9 kJ/mol.

No examples of scaffold C were prepared; however, **51** is an example of a compound having scaffold B (Figure 2). **51** has the same geometry as the compounds shown in Figure 7b and c. While compounds having scaffold B are more potent PI3K α inhibitors they are less potent mTOR inhibitors than compounds having scaffold A. With our aim of making dual mTOR and PI3K α as well as selective mTOR inhibitors, picking scaffold A proved to be the right choice.

4. CONCLUSIONS

Using scaffold hopping we have designed a scaffold for inhibitors of mTOR and PI3 kinases. Optimization, guided by X-ray structures of PI3 kinases and homology models of mTOR, yielded a series of potent inhibitors of these kinases. Utilizing the structural differences between the PI3K α and mTOR ATP-binding site allowed us to design compounds that were dual PI3K and mTOR inhibitors or selective toward mTOR. We do not have X-ray structures of our own compounds, but recently published lipid kinase structures cocrystallized with inhibitors similar to ours have confirmed most of our design hypothesis.^{14,22,31,33,34}

Our inhibitors generally show good PKDM and ADME properties and excellent selectivity in kinase panel screens. The dual mTOR/PI3K inhibitor SB2343 (compound **39**) and the selective mTOR inhibitor SB2602 (compound **46**) were selected for further studies and have progressed to preclinical development. SB2343 has been renamed VS-5584 and is now in a phase I trial in patients with advanced nonhematologic malignancies or lymphoma (NCT01991938).

The work presented here demonstrates how structure-based design coupled with a traditional medicinal chemistry approach can be successfully utilized in the lead generation and lead optimization stages of a drug discovery project and ultimately deliver preclinical candidates.

■ AUTHOR INFORMATION

Corresponding Author

*Phone: +65 6478 8767. Fax: +65 6478 8768. E-mail: apoulsen@etc.a-star.edu.sg. Corresponding author address: Experimental Therapeutics Centre, Agency for Science, Technology and Research, 31 Biopolis Way, Nanos Level 3, Singapore 138669.

Author Contributions

The manuscript was written by Anders Poulsen. All molecular modeling was done by Anders Poulsen. The compounds were conceived of and/or synthesized by Harish Nagaraj, Dizhong Chen, Anders Poulsen, Angeline Lee, Stéphanie Blanchard, Chang Kai Soh, Haishan Wang, Brian Dymock, and Meredith Williams. Biological assays were done by Stefan Hart and Kee Chuan Goh.

Notes

The authors declare no competing financial interest.

■ ABBREVIATIONS

ATP, adenosine triphosphate; DFT, density functional theory; EDTA, ethylenediaminetetraacetic acid; GB/SA, generalized Born/solvent accessible surface; MCMM, Monte Carlo Multiple Minima; MEKi, mitogen-activated protein kinase kinase inhibitors; mTOR, mammalian target of rapamycin; PBF, Poisson–Boltzmann finite element method; PDB, Protein Data Bank; PI3Ks, phosphoinositide 3-kinases; PIKK, phosphatidylinositol 3-kinase-related kinases; PKDM, Pharmacokinetics and Drug Metabolism; PTEN, phosphatase and tensin homologue; RMS, root-mean-square; PRCG, Polak-Ribier Conjugate Gradient; RTKs, receptor tyrosine kinase inhibitors; TNCG, truncated Newton conjugate gradient; TSC1/2, tuberous sclerosis 1/2

■ REFERENCES

- (1) Vanhaesbroeck, B.; Guillermet-Guibert, J.; Graupera, M.; Bilanges, B. The Emerging Mechanisms of Isoform-specific PI3K Signalling. *Nat. Rev. Mol. Cell. Biol.* **2010**, *11*, 329–341.
- (2) Nahta, R.; O'Regan, R. M. Evolving Strategies for Overcoming Resistance to HER2-Directed Therapy: Targeting the PI3K/Akt/mTOR Pathway. *Clin. Breast Cancer* **2010**, *10* (Suppl 3), S72–S78.
- (3) Cully, M.; You, H.; Levine, A. J.; Mak, T. W. Beyond PTEN Mutations: the PI3K Pathway as an Integrator of Multiple Inputs during Tumorigenesis. *Nat. Rev. Cancer* **2006**, *6*, 184–192.

- (4) Ciraolo, E.; Morello, F.; Hirsch, E. Present and Future of PI3K Pathway Inhibition in Cancer: Perspectives and Limitations. *Curr. Med. Chem.* **2011**, *18*, 2674–2685.
- (5) Wee, S.; Jagani, Z.; Xiang, K. X.; Loo, A.; Dorsch, M.; Yao, Y. M.; Sellers, W. R.; Lengauer, C.; Stegmeier, F. PI3K Pathway Activation Mediates Resistance to MEK Inhibitors in KRAS Mutant Cancers. *Cancer Res.* **2009**, *69*, 4286–4293.
- (6) Maestro, LigPrep, MacroModel, Glide & Jaguar; Schrödinger, LLC: New York, NY, 2010.
- (7) Chang, G.; Guida, W. C.; Still, W. C. An Internal-Coordinate Monte Carlo Method for Searching Conformational Space. *J. Am. Chem. Soc.* **1989**, *111*, 4379–4386.
- (8) Jorgensen, W. L.; Maxwell, D. S.; Tirado-Rives, J. Development and Testing of the OPLS All-Atom Force Field on Conformational Energetics and Properties of Organic Liquids. *J. Am. Chem. Soc.* **1996**, *118*, 11225–11236.
- (9) Kaminski, G. A.; Friesner, R. A.; Tirado-Rives, J.; Jorgensen, W. L. Evaluation and Reparametrization of the OPLS-AA Force Field for Proteins via Comparison with Accurate Quantum Chemical Calculations on Peptides. *J. Phys. Chem. B* **2001**, *105*, 6474–6487.
- (10) Hasel, W. H.; Still, W. C. A Rapid Approximation to the Solvent Accessible Surface Areas of Atoms. *Tetrahedron Comput. Methodol.* **1988**, *1*, 103–116.
- (11) Still, W. C.; Tempczyk, A.; Hawley, R. C.; Hendrickson, T. Semianalytical Treatment of Solvation for Molecular Mechanics and Dynamics. *J. Am. Chem. Soc.* **1990**, *112*, 6127–6129.
- (12) Walker, E. H.; Pacold, M. E.; Perisic, O.; Stephens, L.; Hawkins, P. T.; Wymann, M. P.; Williams, R. L. Structural Determinants of Phosphoinositide 3-kinase Inhibition by Wortmannin, LY294002, Quercetin, Myricetin, and Staurosporine. *Mol. Cell* **2000**, *6*, 909–919.
- (13) Huang, C. H.; Mandelker, D.; Schmidt-Kittler, O.; Samuels, Y.; Velculescu, V. E.; Kinzler, K. W.; Vogelstein, B.; Gabelli, S. B.; Amzel, L. M. The Structure of a Human p110alpha/p85alpha Complex Elucidates the Effects of Oncogenic PI3Kalpha Mutations. *Science* **2007**, *318*, 1744–1748.
- (14) Berndt, A.; Miller, S.; Williams, O.; Le, D. D.; Houseman, B. T.; Pacold, J. I.; Gorrec, F.; Hon, W. C.; Liu, Y.; Rommel, C.; Gaillard, P.; Ruckle, T.; Schwarz, M. K.; Shokat, K. M.; Shaw, J. P.; Williams, R. L. The p110 delta Structure: Mechanisms for Selectivity and Potency of new PI(3)K Inhibitors. *Nat. Chem. Biol.* **2010**, *6*, 117–124.
- (15) Trésaugues, L.; Arrowsmith, C. H.; Berglund, H.; Bountra, C.; Collins, R.; Edwards, A. M.; Flodin, S.; Flores, A.; Graslund, S.; Hammarstrom, M.; Johansson, I.; Karlberg, T.; Kotenyova, T.; Kraulis, P.; Moche, M.; Nordlund, P.; Nyman, T.; Persson, C.; Schueler, H.; Schutz, P.; Siponen, M. I.; Thorsell, A. G.; Tresaugues, L.; Van Den Berg, S.; Wahlberg, E.; Weigelt, J.; Welin, M.; Wisniewska, M. Crystal Structure of Human PIK3C3 in Complex with 3-[4-(4-Morpholinyl)-thieno[3,2-d]pyrimidin-2-yl]-phenol. *Protein Data Bank* **2010**, PDB-ID 3LS8.
- (16) Berman, H. M.; Westbrook, J.; Feng, Z.; Gilliland, G.; Bhat, T. N.; Weissig, H.; Shindyalov, I. N.; Bourne, P. E. The Protein Data Bank. *Nucleic Acids Res.* **2000**, *28*, 235–242.
- (17) Bostrom, J.; Norrby, P. O.; Liljefors, T. Conformational Energy Penalties of Protein-Bound Ligands. *J. Comput.-Aided Mol. Des.* **1998**, *12*, 383–396.
- (18) Consortium, T. U. The Universal Protein Resource (UniProt) in 2010. *Nucleic Acids Res.* **2009**, *38*, D142–148.
- (19) Chenna, R.; Sugawara, H.; Koike, T.; Lopez, R.; Gibson, T. J.; Higgins, D. G.; Thompson, J. D. Multiple Sequence Alignment with the Clustal Series of Programs. *Nucleic Acids Res.* **2003**, *31*, 3497–3500.
- (20) Jones, D. T. Protein Secondary Structure Prediction Based on Position-Specific Scoring Matrices. *J. Mol. Biol.* **1999**, *292*, 195–202.
- (21) Pollastri, G.; Przybylski, D.; Rost, B.; Baldi, P. Improving the Prediction of Protein Secondary Structure in Three and Eight Classes Using Recurrent Neural Networks and Profiles. *Proteins* **2002**, *47*, 228–235.
- (22) Yang, H.; Rudge, D. G.; Koos, J. D.; Vaidialingam, B.; Yang, H. J.; Pavletich, N. P. mTOR Kinase Structure, Mechanism and Regulation. *Nature* **2013**, *497*, 217–23.
- (23) Tannor, D. J.; Marten, B.; Murphy, R.; Friesner, R. A.; Sitkoff, D.; Nicholls, A.; Honig, B.; Ringnalda, M.; Goddard, W. A. Accurate First Principles Calculation of Molecular Charge Distributions and Solvation Energies from Ab Initio Quantum Mechanics and Continuum Dielectric Theory. *J. Am. Chem. Soc.* **1994**, *116*, 11875–11882.
- (24) Nagaraj, H. K. M.; Chen, D.; Poulsen, A.; Williams, A. 2-Morpholinylpurines as Inhibitors of PI3K. PCT/SG2008/000378, Oct. 3, 2008.
- (25) GraphPad Prism, version 5; GraphPad Software: La Jolla, CA, 2011.
- (26) Athar, U.; Gajra, A. Role of mTOR in Hematological Malignancies. *Curr. Cancer Ther. Rev.* **2008**, *4*, 211–218.
- (27) Fuchikami, K.; Togame, H.; Sagara, A.; Satoh, T.; Gantner, F.; Bacon, K. B.; Reinemer, P. A Versatile High-Throughput Screen for Inhibitors of Lipid Kinase Activity: Development of an Immobilized Phospholipid Plate Assay for Phosphoinositide 3-Kinase gamma. *J. Biomol. Screening* **2002**, *7*, 441–450.
- (28) Hayakawa, M.; Kaizawa, H.; Moritomo, H.; Koizumi, T.; Ohishi, T.; Yamano, M.; Okada, M.; Ohta, M.; Tsukamoto, S.; Raynaud, F. I.; Workman, P.; Waterfield, M. D.; Parker, P. Synthesis and Biological Evaluation of Pyrido[3',2':4,5]furo[3,2-d]pyrimidine Derivatives as Novel PI3 Kinase p110alpha Inhibitors. *Bioorg. Med. Chem. Lett.* **2007**, *17*, 2438–2442.
- (29) Vlahos, C. J.; Matter, W. F.; Hui, K. Y.; Brown, R. F. A Specific Inhibitor of Phosphatidylinositol 3-Kinase, 2-(4-Morpholinyl)-8-phenyl-4H-1-benzopyran-4-one (LY294002). *J. Biol. Chem.* **1994**, *269*, 5241–5248.
- (30) Yaguchi, S.; Fukui, Y.; Koshimizu, I.; Yoshimi, H.; Matsuno, T.; Gouda, H.; Hiroto, S.; Yamazaki, K.; Yamori, T. Antitumor Activity of ZSTK474, a New Phosphatidylinositol 3-Kinase Inhibitor. *J. Natl. Cancer Inst.* **2006**, *98*, 545–556.
- (31) Zhao, Y.; Zhang, X.; Chen, Y.; Lu, S.; Peng, Y.; Wang, X.; Guo, C.; Zhou, A.; Zhang, J.; Luo, Y.; Shen, Q.; Ding, J.; Meng, L. Crystal Structures of PI3Kalpha Complexed with PI103 and Its Derivatives: New Directions for Inhibitors Design. *ACS Med. Chem. Lett.* **2014**, *5*, 138–142.
- (32) Miller, S.; Tavshanjian, B.; Oleksy, A.; Perisic, O.; Houseman, B. T.; Shokat, K. M.; Williams, R. L. Shaping Development of Autophagy Inhibitors with the Structure of the Lipid Kinase Vps34. *Science* **2010**, *327*, 1638–1642.
- (33) Sutherlin, D. P.; Sampath, D.; Berry, M.; Castanedo, G.; Chang, Z.; Chuckowree, I.; Dotson, J.; Folkes, A.; Friedman, L.; Goldsmith, R.; Heffron, T.; Lee, L.; Lesnick, J.; Lewis, C.; Mathieu, S.; Nonomiya, J.; Olivero, A.; Pang, J.; Prior, W. W.; Salphati, L.; Sideris, S.; Tian, Q.; Tsui, V.; Wan, N. C.; Wang, S.; Wiesmann, C.; Wong, S.; Zhu, B. Y. Discovery of (Thienopyrimidin-2-yl)aminopyrimidines as Potent, Selective, and Orally Available Pan-PI3-Kinase and Dual Pan-PI3-Kinase/mTOR Inhibitors for the Treatment of Cancer. *J. Med. Chem.* **2010**, *53*, 1086–1097.
- (34) Ohwada, J.; Ebiike, H.; Kawada, H.; Tsukazaki, M.; Nakamura, M.; Miyazaki, T.; Morikami, K.; Yoshinari, K.; Yoshida, M.; Kondoh, O.; Kuramoto, S.; Ogawa, K.; Aoki, Y.; Shimma, N. Discovery and Biological Activity of a Novel Class I PI3K Inhibitor, CHS132799. *Bioorg. Med. Chem. Lett.* **2011**, *21*, 1767–1772.
- (35) Zask, A.; Kaplan, J.; Verheijen, J. C.; Richard, D. J.; Curran, K.; Brooijmans, N.; Bennett, E. M.; Toral-Barza, L.; Hollander, I.; Ayrak-Kaloustian, S.; Yu, K. Morpholine Derivatives Greatly Enhance the Selectivity of Mammalian Target of Rapamycin (mTOR) Inhibitors. *J. Med. Chem.* **2009**, *52*, 7942–795.
- (36) Hart, S.; Novotny-Diermayr, V.; Goh, K. C.; Williams, M.; Tan, Y. C.; Ong, L. C.; Cheong, A.; Ng, B. K.; Amalini, C.; Madan, B.; Nagaraj, H.; Jayaraman, R.; Pasha, K. M.; Ethirajulu, K.; Chng, W. J.; Mustafa, N.; Goh, B. C.; Benes, C.; McDermott, U.; Garnett, M.; Dymock, B.; Wood, J. M. VS-5584, a Novel and Highly Selective

PI3K/mTOR Kinase Inhibitor for the Treatment of Cancer. *Mol. Cancer Ther.* **2013**, *12*, 151–161.